

A METHOD FOR GENERATING PLANE WAVE AND ZERO-OFFSET VSP SYNTHETIC SEISMOGRAMS

by

Suprajitno Munadi

ABSTRACT

Synthetic Vertical Seismic Profiles (VSP) seismograms are a useful aid to the interpretation of VSP records. Plane wave VSP synthetics which accommodate multiples and mode conversions can be computed rapidly in the frequency domain using a new recursive formulation.

The method utilises the concept of "resultant" phase related reflection and transmission coefficients for a layer stack. High frequency signals can be handled with relative ease. The ability to control the order of the multiple avoids wraparound problems with the discrete Fourier transform. Several examples are used to illustrate the method with relevance to seismic exploration.

I. INTRODUCTION

The concern in this paper is with a rapid, accurate method for computing plane wave synthetic VSP seismograms. In analysing real data, synthetic seismograms are an indispensable aid to interpretation. They are very instructive in their own right for understanding the form and appearance of the VSP record. A modelling capability also provides a powerful means to check the effectiveness of the various data processing steps.

Over the past few years several different approaches have been introduced to generate theoretical VSP seismograms. Most assume a plane layered earth and are restricted to the zero-offset normal incidence case.

Vetter (1980) introduced a raypath approach with claimed economy of computer storage and time. He used a wavelet labelling and enumeration system for specification of all the dynamically equivalent rays. As the number of layers (and possible rays) increases, the system becomes quite complicated.

Wyatt (1981) introduced a normal incidence formulation based on the state space model (Mendel,

1978). In his approach the model is artificially divided into N layers, each having equal one way travel time (Goupillaud, 1961; Claerbout, 1968).

The finite difference method (Kelly, Alford and Whitmore, 1982) has proved to be very successful, but it is time consuming and expensive, particularly for computations in the far-field. Gridding artifacts, such as fictitious signal dispersion, can arise with finite difference schemes.

More recently Ursin and Arntsen (1983) proposed a computation method based on the application of the ray series to the Fourier transform of the equations of motion for a linear visco-elastic model. This method is only applicable to the compressional wave, normal incidence case.

Thybo (1983) presented a fast computation method for earth structures comprising equal travel time layers using an iterative calculation procedure, arranged like a binary tree. A matrix describing N layers is represented by a one dimensional spectrum with N complex samples. At each step of the iteration scheme, layers are combined in pairs, and the resulting spectrum of double length is computed for each pair. He restricts his attention to the zero offset case and

uses a computation convenience introduced by Choate (1982).

The method developed here utilises the concept of "resultant" reflection and transmission coefficients for multilayered media above and below the level of the receiver.

The VSP geometry is illustrated in Figure 1. The diagram shows the direct arrival and several primary and multiple reflections. With the receiver R at depth, both upgoing and downgoing waves must be considered.

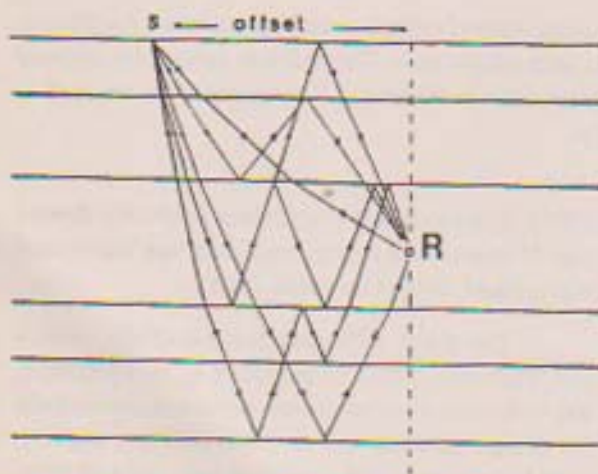


Figure 1.
"Resultant" Reflection and Transmission
Coefficients at R

Calculations are performed in the frequency domain in using an exact, recursive formulation. Surface multiples as well as internal multiples can be easily generated. Moreover the order of the multiple can also be controlled. Our method shares some similarities with that of Thybo (1983) but it is more general in that mode conversion and plane wave incidence angle can be taken into account. In a separate paper (Suprajitno and Greenhalgh, 1984) we present a formal solution for the offset VSP point source (spherical wave) theoretical seismogram problem.

II. THEORETICAL DEVELOPMENT

A. Background

To compute the seismic response of a layered medium the frequency domain approach, pioneered by Thomson (1950) and Haskell (1953), is widely used. In this approach the solution of the wave equations in every layer are expressed in terms of the Fourier transform of the displacement potentials. As the waves propagate outward from the source, the stresses and displacements are continuous across the layers as well as across the various interfaces. This continuity enables us to express the stresses and displacements in the n^{th} layer in terms of the stresses and displacements in layer 1. At every interface there are five possible wave types to consider: the incident wave (P or S), the transmitted P and S waves, and the reflected P and S waves. A formidable matrix book-keeping operation is required in repeatedly applying the continuity conditions.

The extension of the Haskell-Thomson matrix approach has been discussed in a number of papers (e.g., Knopoff, 1965; Dunkin, 1965; Fuchs, 1968; Kind, 1976), principally to overcome some numerical instabilities in the matrix inversion and to speed-up the computations. Gilbert and Backus (1966), starting from a different approach, generalised the formula for transferring stresses and displacements between two levels in a stack of layers. They introduced the concept of propagator matrices (Aki and Richards, 1980, p. 273 - 283).

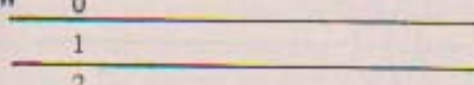
The solution of the wave equations which satisfy the boundary (or continuity) conditions enables us to express the boundary conditions in terms of the reflection and transmission coefficients (Brekhovskikh, 1960, p. 405). In other words, their solution at each interface leads to the definition of the reflection and transmission coefficients associated with that interface (Robinson, 1968). Kennett (1974), using Gilbert - Backus propagator matrices, established the connection between the Thomson - Haskell approach and the reflection and transmission properties of a single interface. He then used this inter-relationship

to combine reflection and transmission coefficients of two interfaces (an embedded layer) into that of a single equivalent boundary.

B. Overall Reflection and Transmission Coefficients

Consider the case of a downgoing plane wave incident on layer 1 in Figure 2(a). We can combine the individual coefficients from the top boundary (R^{01} and T^{01}) with those of the bottom boundary (R^{12} and T^{12}) into the resultant coefficients for the layer, as given in Figure 2(a). The D and U subscripts denote either downgoing or upgoing waves. Similar results apply for a wave incident from below [Figure 2(b)] but the individual coefficients in this case correspond to the direction of an upgoing wave. Note that the square bracket term appearing in Figure 2 can be expanded in a Taylor series with the individual terms in the series corresponding to the various multiples. Truncation of the series at a specified location controls the order of the multiple. If only the first term is retained then we have the "primaries only" response of the layer, i.e., a single reflection from top of the layer.

UGW

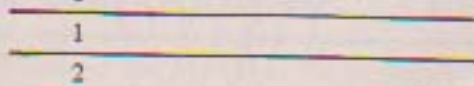


$$R_U = R_U^{12} + T_U^{12} \cdot R_U^{01} \left[1 - R_D^{12} \cdot R_U^{01} \right]^{-1} \cdot T_D^{12}$$

$$T_U = T_U^{12} \left[1 - R_D^{12} \cdot R_U^{01} \right]^{-1} \cdot T_U^{01}$$

Figure 2(a).

DGW



$$R_D = R_D^{01} + T_D^{01} \cdot R_D^{12} \left[1 - R_D^{12} \cdot R_U^{01} \right]^{-1} \cdot T_U^{01}$$

$$T_D = T_D^{01} \left[1 - R_D^{12} \cdot R_U^{01} \right]^{-1} \cdot T_D^{12}$$

Figure 2(b).

The individual reflection and transmission coefficients can be computed from the well known Zoeppritz and Knott equations (Pilant, 1979, p. 130, 137). They are complicated functions of the wave incidence angle and the elastic parameters of the model (viz. P and S velocities, and densities). It is possible to repeatedly combine reflection/transmission coefficients at successive interfaces to yield overall coefficients for the complete layer stack. Figure 3(a) shows the resultant transmission/reflection coefficients in terms of the rays for downgoing waves between layers m and L . In computing the overall coefficients (${}^m(R_D)^L$ and ${}^m(T_D)^L$) we recursively combine two interfaces into one starting at the top of the stack and working our way down or vice versa. Figure 3(b) shows the corresponding ray diagram and definition of resultant coefficients for an upgoing wave incident from layer L .

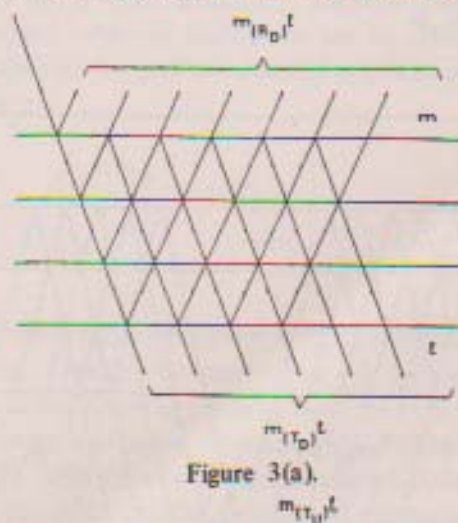


Figure 3(a).

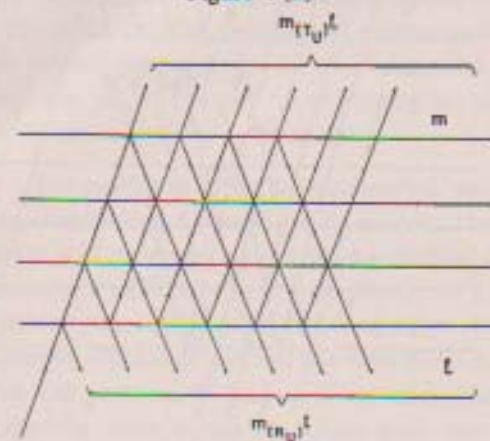


Figure 3(b).

C. Basic Formula

Consider a plane wave which impinges on top of layer m within a stack of layers from m to n . (Figure 4). Suppose that the receiver is located at an arbitrary level l . The incident wave gives rise to upgoing P and S waves as well as downgoing P and S waves in all layers (except in layer n where only downgoing waves exist).

The amplitude of the displacement potential at l will depend on three factors :

1. The overall transmission coefficient for downgoing waves from layer m to layer l , expressed as ${}^m(T_D)^l$
2. The overall reflection coefficient from downgoing waves from layer l to layer n , expressed as ${}^l(R_D)^n$

3. The overall reflection coefficient for upgoing waves from layer l to layer m , expressed as ${}^m(R_U)^l$.

These terms are Kennett's matrices and they are calculated along the lines indicated in Figures 2 and 3. Mode conversion can be included by considering the individual elements of the R and T matrices.

$$R_D = \begin{pmatrix} R_{PP}^D & R_{PS}^D \\ R_{SP}^D & R_{SS}^D \end{pmatrix} \quad T_D = \begin{pmatrix} T_{PP}^D & T_{PS}^D \\ T_{SP}^D & T_{SS}^D \end{pmatrix}$$

$$R_U = \begin{pmatrix} R_{PP}^U & R_{PS}^U \\ R_{SP}^U & R_{SS}^U \end{pmatrix} \quad T_U = \begin{pmatrix} T_{PP}^U & T_{PS}^U \\ T_{SP}^U & T_{SS}^U \end{pmatrix}$$

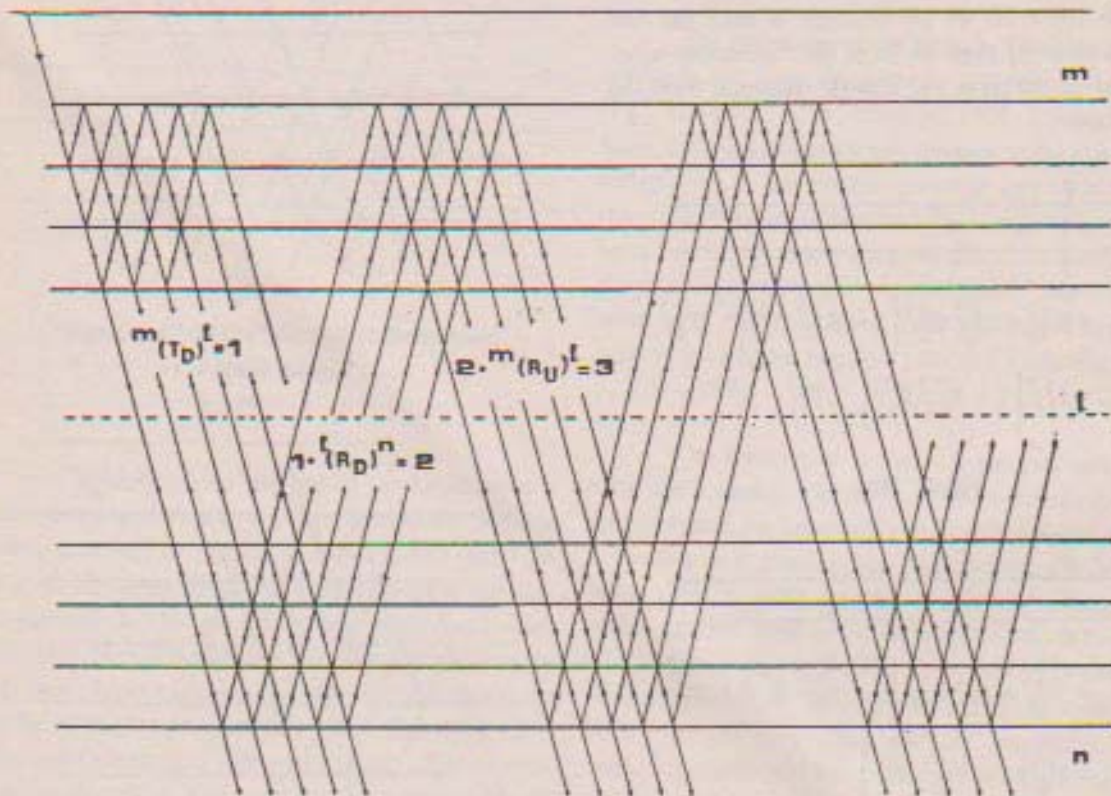


Figure 4.

where D and U represent and downgoing and upgoing waves respectively.

The resultant reflection and transmission coefficients for the receiver within layer \mathcal{L} can be expressed in terms of these matrices as follows: (1)

$$R_T = {}^m(T_D)^{\mathcal{L}} [1 + {}^{\mathcal{L}}(R_D)^n] [1 - {}^{\mathcal{L}}(R_D)^n {}^m(R_U)^{\mathcal{L}}]^{-1}$$

This formula includes the contributions of all possible rays to the particle displacement. Terms within the large bracket which are under the minus sign represent the multiply reflected waves within layer \mathcal{L} . Controlling the order of the multiple is effected by binomial expansion and retaining the appropriate number of terms. The coefficients R and T are phase related to receiver's level within layer \mathcal{L} (see Scholte, 1956; Cisternas et al., 1973; Kennett, 1979). The advantage of using these phase-related coefficients is that the layer's travel times have already been carried by the coefficients themselves. These travel times are not restricted to having to be equal, an artifice used in the usual z-transform normal - incidence approach (e.g., Goupilaud, 1961; Claerbout, 1968).

The actual seismograms are obtained by multiplying R_T by the spectrum of the signal, then followed by inverse Fourier transformation. Equation (1) requires modification for including the free surface reflection effect. The relevant equation is given in Appendix. Also included in the Appendix are the formulations for three special cases of location of the receiver: on the surface, within the first layer, and within the half-space (transmitting zone).

D. Offset Plane Wave VSP

The resultant coefficients given by equation (1) are the plane wave coefficients for a given incidence angle (or horizontal wave number). The vertical component of the delay times due to the passage of the waves across the layers are computed by:

$$t_{pi} = \frac{h_i}{V_{pi}} \cos \theta_{pi}$$

and $t_{si} = \frac{h_i}{V_{si}} \cos \theta_{si}$ (2)

where h_i is the thickness of the i^{th} layer, V_{pi} is the P-wave velocity, V_{si} is the S-wave velocity, and θ_{pi} and θ_{si} are the corresponding P and S wave incidence angles respectively.

If X is the horizontal distance between the receiver and the borehole, the horizontal component of the delay time can be computed using:

$$t_{hp} = \frac{X}{V_{pi}} \sin \theta_{pi} = \frac{X}{C_p}$$

and $t_{hs} = \frac{X}{V_{si}} \sin \theta_{si} = \frac{X}{C_s}$ (3)

where C_p and C_s are the horizontal phase velocities for P and S waves respectively. The offset plane wave resultant reflection coefficients can be obtained by multiplying the previous resultant coefficients by the matrix:

$$\begin{pmatrix} e^{-j\omega t_{hp}} & 0 \\ 0 & e^{-j\omega t_{hs}} \end{pmatrix}$$

The result follows from the work of Aminzadeh and Mendel (1982), who showed that the seismogram at any offset X can be obtained from the "non-normal incidence zero-offset" seismogram by shifting the received signal by an amount X/C where C is the phase velocity. Note that the definition of non-normal incidence zero-offset seismogram used by Aminzadeh and Mendel (op. cit.) is the zero offset seismogram whose travel times are given by equation (2).

For generating offset point source VSP seismograms, (Figure 5) plane waves can be integrated over a wide range of incidence angle to form a spherical wave (Summerfeld, 1909; Weyl, 1919; Stephen, 1977). In a companion paper (Suprajitno and Greenhalgh, 1984) we present a practical method for solving the point source VSP problem. In the case of normal incidence, the spherical wave equals the plane wave, and the point source solution reduces to equation (1).

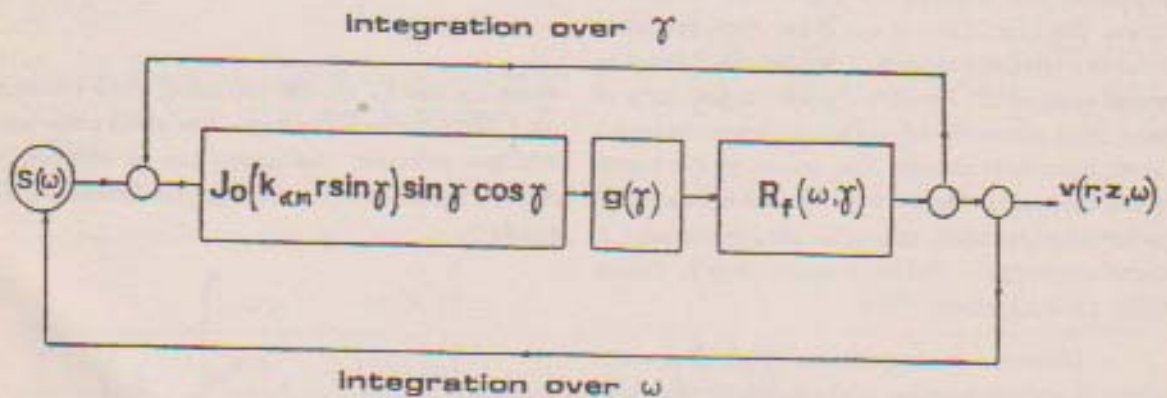
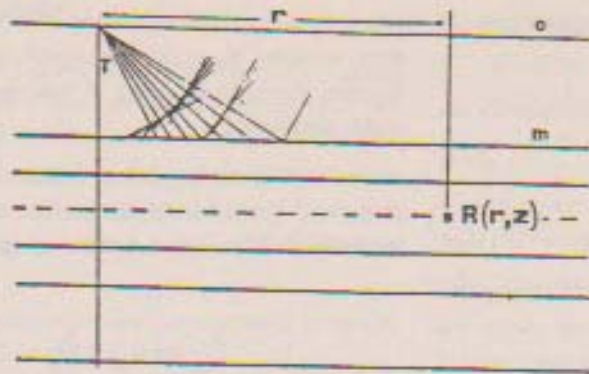


Figure 5.

E. Synthetic Examples

In this section we demonstrate the use of the above coefficients for generating zero-offset VSP synthetic seismograms for a small number of models of potential significance in exploration.



Figure 6.

The choice of a source signal is arbitrary. For convenience we use a short tone burst such as shown in Figure 6. With this source, one is free to specify dominant frequency and the number of cycles.

F. A Single Embedded Layer

Figure 7 shows the compressional wave VSP synthetics calculated at 21 different levels of the receiver using an increment of 10 m. The velocity model, which comprises a single embedded high speed layer is shown on the left of the diagram. Points indicate positions of the receiver. Depth runs vertically downwards and time increases to the right. A source signal with a dominant frequency of 100 Hz is used. The sample rate is 0.5 milliseconds.

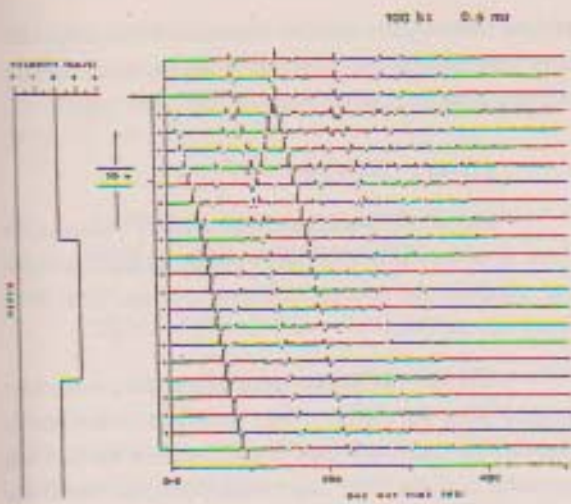


Figure 7.

The seismograms display the downgoing wave and the primary reflections from both interfaces. The moveout pattern on the first arrivals reflects the subsurface velocity distribution. The upgoing waves (reflections) are characterised by a negative apparent velocity i.e. time increases with decreasing depth. Note how the upgoing primary reflections and the first downgoing wave intersect at the two interface - thus providing a means of locating them.

We observe a phase reversal on the second (deeper) reflection due to the velocity decrease in the basal layer. The form of the signal has been conserved.

Surface multiples and internal multiples can be seen quite clearly on the display. Any event which disappears or terminates in the general record before reaching the first breaks is a multiple. The display resembles a ray picture in the subsurface. (See also Suprajitno and Greenhalgh, 1983). It is easy to trace the origin of all events on the record in terms of their ray-paths.

Our display has been constructed in such a way that each trace is normalised to its maximum. Furthermore, a linear ramp has been applied to enhance the later arrivals. For geophone positions below the level of the basal interface no upgoing waves can be observed.

The top three traces are normal-incidence surface source-surface receiver seismograms. They contain only the upgoing waves. Numerous multiples are present on the traces.

G. Four Layer Case

Figure 8 shows the theoretical VSP seismograms for a slightly more complicated model. The geophone spacing is 25 m and the source signal has a dominant frequency of 60 Hz. The sample rate is 1 millisecond. Note the presence of primary reflections from each interface. The upgoing and downgoing waves intersect at the three levels. We can clearly correlate the surface seismograms with the VSP and trace all events down to their points of origin. Multiples are again well developed and easy to identify on the display. There are several orders of multiples present. The downgoing waves are strong in amplitude compared to the upgoing waves, even without making allowance for the time varying gain function applied.

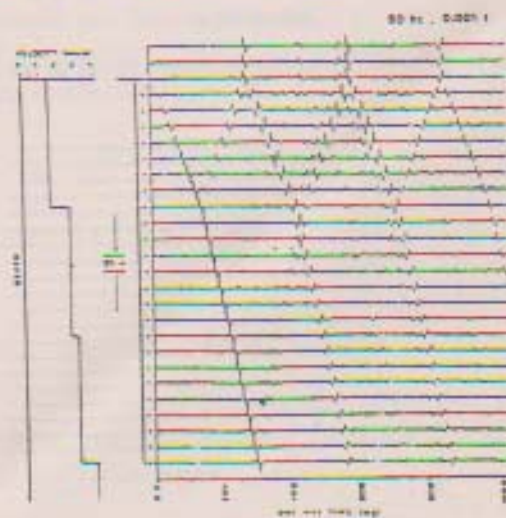


Figure 8.

H. Multilayers - Prediction Ahead of the Drill Bit

This example, shown in Figure 9(a), includes many more layers, with layering below the terminal depth of the well. It serves to demonstrate how VSP can be used to map structure ahead of the bit. In Figure 9(b) we observe upgoing waves (negative apparent

velocity) which have not intersected the first breaks on traces at the base of the well. These events can be extrapolated in depth to locate the reflector levels.

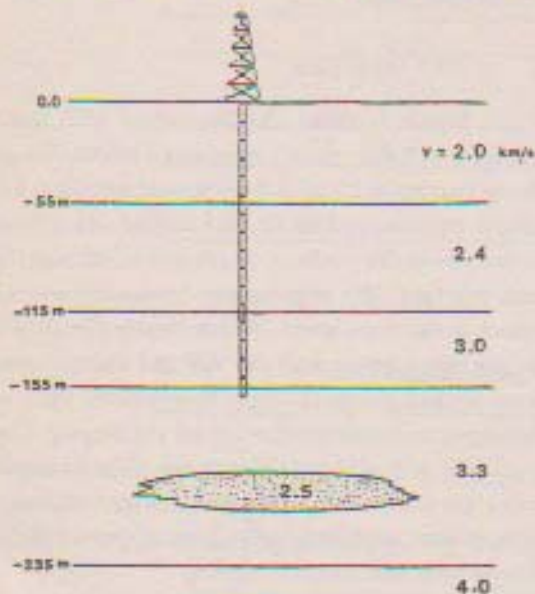


Figure 9(a).

The low velocity sand lens structure ahead of the bit

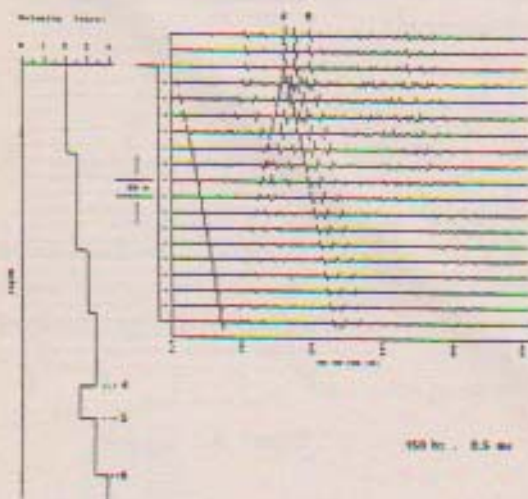


Figure 9(b).

There is a phase change evident on the surface trace at position 4, corresponding to the top of the low velocity layer. Reflections 5 and 6, from below the zone, are of normal polarity. Much of the energy

at late time on the surface traces is of a multiple nature. Increasing the number of layers even further, produces quite a complicated set of seismograms.

I. Primary - Multiple Interference

Figure 10 is included as a seismic curiosity, to show how interaction between primaries and multiples can confuse the interpretation of conventional (surface) seismic data.

The first multiple from interface 1 coincides in time with the primary from interface 2. The multiple, having been reflected from the free surface has opposite polarity. The two events perfectly cancel for receivers above the interface level. However, the primary can be identified on the VSP traces below the level of interface 1. Automatic Gain Control has been applied to these particular traces.

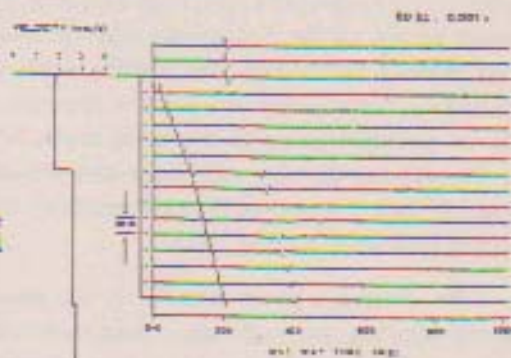


Figure 10.

III. CONCLUSIONS

We have presented a simple and practical method for generating theoretical VSP seismograms. The method is based on the recursive determination of the resultant phase-related reflection and transmission coefficients for a layer-stack. The flexibility in accepting models with different layer travel times reduces the required memory and computer time. The possibility of controlling the order of the multiples avoids aliasing and wraparound problems (Trorey, 1962, p. 769). The method can be extended to offset VSP, even where the angle of incidence exceeds the critical angle

and the reflection transmission coefficients become complex. Absorption can be included by using complex velocities. High frequency signals can be handled with relative ease.

IV. APPENDIX SPECIAL CASES FOR RESULTANT COEFFICIENTS

A. Effect of Free-Surface Reflection

Equation (1) does not include the effect of the free surface reflection. This effect can easily be accommodated by writing (See Suprajitno, 1985 for derivation of this and following equations).

$$R_f' = e^{-j\omega t_1} [R_f + {}^m(T_D)^k \{1 + {}^k(R_D)^n\} \sum_{i=1}^M A^i]$$

where $A = r_{FS} {}^m(R_D)^n E^2$

$$\text{with } r_{FS} = \begin{pmatrix} r_{PP} & r_{PS} \\ r_{SP} & r_{SS} \end{pmatrix}$$

$$E = \begin{pmatrix} e^{-j\omega t_P} & 0 \\ 0 & e^{-j\omega t_S} \end{pmatrix}$$

Here R_f' is the resultant coefficient which includes the free surface reflection, R_f is given by equation (1), T_1 is the one way travel time from the surface to the first interface, M is the order of the free surface multiples, t_P and t_S are the travel times of P and S waves in layer 1, and r_{PP} , r_{PS} , r_{SP} and r_{SS} are the free surface reflection coefficients. Equations for r_{FS} can be found in Pilant (1979, p. 82-89).

B. Receiver on the Surface

For the case of the receiver located on the free surface it is obvious that the resultant coefficients only consists of the overall upgoing wave from layers bounded by layer m to n (layer m is the surface layer). The resultant coefficient can be written as :

$$R_f'' = {}^m(R_D)^n e^{-j2\nu_m h} \sum_{i=0}^M A^i \quad (\text{A. 2})$$

where $A = {}^m(R_D)^n R_{FS}$

$$R_{FS} = r_{FS} e^{-j2\nu_m h}$$

Note that ν_m is vertical wave number given by :

$$\nu_m h = \omega T_1$$

The terms r_{FS} and M are those defined above.

C. Receiver in the First Layer

The first layer in Figure 4 is layer m since it is bounded above by the Earth's free surface. A receiver located at a given level within this layer records both the upgoing waves as well as the downgoing waves. The upgoing waves are composed of the primary reflections plus the multiply reflected waves from the stack of layers between m and n . The downgoing waves are composed of the direct wave from the source plus the free surface multiples. If h_1 is the thickness of the first layer then it can be shown that the resultant coefficient is given by :

$$R_f''' = e^{-j\nu_m h_1} \left[1 + {}^m(R_D)^n \right] \sum_{i=0}^M A^i \quad (\text{A. 3})$$

where $A = {}^m(R_D)^n r_{FS} e^{-j\nu_m h_1}$

D. Receiver within the Basement

The resultant coefficient for the case of the receiver within the basement (half-space or transmitting zone) is given by :

$$R_f^{(iv)} = e^{-j\nu_m h} {}^m(T_D)^n \sum_{i=0}^M (A)^i \quad (\text{A. 4})$$

where $A = {}^m(R_D)^n r_{FS}$

Here h is the thickness of the layer m , M is the order of the free surface multiple, and r_{FS} is the free-surface reflection coefficient : All coefficients are phase related to the receiver's level in layer n .

REFERENCES

- Aki, K. and Richard, P.G., *Quantitative seismology, vol. 1, Theory and Methods*, W.H. Freeman, San Francisco, 1980.
- Aminzadeh, F. and Mendel, J.M., *Non-normal incidence state space model and line source reflection synthetic seismogram*, *Geophysical Prospecting* 30, 541-568, 1982.
- Claerbout, J.F., *Synthesis of a layered medium from its acoustic transmission response*, *Geophysics*, 33, 264-269, 1968.
- Dunkin, J.W., *Computation of model solutions in layered elastic media at high frequencies*, *Bulletin of the Seismological Society of America* 55, 335-358, 1965.
- Fuchs, K., *The reflectivity and transmittance of a stratified medium with variable depth distribution of models of elasticity and density for inclined incidence of planewaves*, Translated from *Zeitschrift für Geophysik* 34, 389-411 by E.H. FEEken, Bureau of Mineral Resources, Canberra, 1968.
- Goupillaud, P., *An approach to inverse filtering of the near surface layer effect from seismic records*, *Geophysics* 26, 754-760, 1961.
- Gilbert, F. and Backus, G.E., *Propagator matrices in elastic wave and vibration problems*, *Geophysics* 31, 326-332, 1966.
- Haskell, N.A., *The dispersion of surface waves on multilayered media*, *Bulletin of the Seismological Society of America* 43, 17-34, 1953.
- Kennett, B.L.N., *Reflections, rays and reverberations*, *Bulletin of the Seismological Society of America* 64, 1685-1696, 1974.
- Kennett, B.L.N., *Theoretical reflection seismogram for elastic media*, *Geophysical Prospecting* 27, 301-321, 1979.
- Knopoff, L., *A matrix method for elastic wave problems*, *Bulletin of Seismological Society of America* 54, 431-438, 1964.
- Kind, R., *Computation of reflection coefficients for layered media*, *Journal of Geophysics* 42, 191-200, 1976.
- Pilant, W.L., *Elastic wave in the earth*, Elsevier, Amsterdam, 1979.
- Robinson, E.A., *Basic equation for synthetic seismogram using z transform approach*, *Geophysics* 33, 521-523, 1968.
- Scholte, J.G.J., *On seismic waves in a spherical Earth*, *Koninkl. Nederland Meteorol. Institute* 65, 1-55, 1956.
- Sommerfeld, A., *Über die Ausbreitung der Wellen in der draht losen Telegraphie*, *Ann. Physik* 28, 665-736.
- Suprajitno, M., *Vertical Seismic Profiling : numerical simulation, data processing and analysis*, Ph.D. Thesis, Flinders University of South Australia, 1985.
- Suprajitno, M. and Greenhalgh, S.A., *Vertical Seismic Profiling : drawing rays beneath the Earth's surface*, Presented at 3rd Biennial Conference of Australia Society of Exploration Geophysicists, Brisbane, October 31 - November 4, 1983.
- Suprajitno, M. and Greenhalgh, S.A., *Offset VSP theoretical seismogram computation*, Submitted to *Geophysics*, 1984.
- Temme, P. and Mueller, G., *Numerical simulation of Vertical Seismic Profiling*, *Journal of Geophysics* 50, 177-188, 1982.
- Thybo, H., *Fast computation of synthetic Vertical Seismic Profiles*, Presented at the 45th Annual Meeting of the EAEG, Oslo, June 14 - 17, 1983.
- Trorey, A., *Theoretical seismogram with frequency and depth dependent absorption*, *Geophysics* 27, 766-785, 1962.

Vetter, W.J., *A ray path reflection model for layered media with source and receiver in different layers*, IEEE International Conference on Acoustic, Speech and Signal Processing, 103–106, 1980.

Ursin, B. and Arnsten, B., *Computation of zero-offset Vertical Seismic Profile including spherical spreading and absorption*, Presented at the

45th meeting of the EAEG, Oslo, June 14–17, 1983.

Wyatt, K.D., *Synthetic Vertical Seismic Profile*, Geophysics 46, 880–891, 1981.

Weyl, H., *Ausbreitung elektromagnetischer Wellen umher einen Leiter*, Ann. Physik 60, 481–500, 1919.

LIST OF FIGURES

Fig. 1. Source-receiver geometry for offset VSP. The receiver R is moved vertically down the borehole. The diagram shows several raypaths (upgoing and downgoing waves) arriving at R.

Fig. 2. The overall phase related reflection and transmission coefficients R and T for a single embedded layer. Diagram (a) is for the case of a downgoing wave (DGW) incident on interface 0:1. Diagram (b) is for the case of an upgoing wave (UGW) incident from below an interface 2:1.

Fig. 3. A ray interpretation of the overall reflection and transmission coefficients for a layer stack. The coefficients accommodate all orders of multiple reflections within the structure. The two diagrams correspond to (a) downgoing wave incident from layer m (b) upgoing wave incident from layer ℓ .

Fig. 4. The resultant coefficient at level ℓ depends on the three overall coefficients ${}^m(T_D)_{\ell}^{\ell}$, ${}^{\ell}(R_D)^n$ and ${}^m(R_D)_{\ell}^{\ell}$. Only several of the infinite family of possible rays are shown.

Fig. 5. Point source (spherical wave) synthetic seismograms can be obtained by integrating the plane wave response function.

Fig. 6. The source function used in the synthetic seismogram computations.

Fig. 7. Normal incidence synthetic VSP seismograms for a single embedded high speed layer. Primaries and multiple reflections can be easily identified. The diagram resembles a ray picture in the subsurface.

Fig. 8. VSP synthetic seismograms for a four-layer case.

Fig. 9(b). Multilayer VSP synthetics illustrating prediction ahead of the bit. Upgoing events 4, 5 and 6 which have not intersected the first breaks on traces of the base of the well, represent primary reflections from layering below the terminal depth of the hole.

Fig. 10. Synthetic VSP traces showing primary-multiple interaction. The surface multiple cancels out the primary reflection from the basal interface.